

Neutrinoless Double Beta Decay, the Inverted Hierarchy and Precision Determination of θ_{12}

Alexander Dueck^{a*}, Werner Rodejohann^{a†}, Kai Zuber^{b‡}

^a*Max-Planck-Institut für Kernphysik,
Postfach 103980, D-69029 Heidelberg, Germany*

^b*Technische Universität Dresden,
Institut für Kern- und Teilchenphysik,
D-01069 Dresden, Germany*

Abstract

Ruling out the inverted neutrino hierarchy with neutrinoless double beta decay experiments is possible if a limit on the effective mass below the minimal theoretically possible value is reached. We stress that this lower limit depends strongly on the value of the solar neutrino mixing angle: it introduces an uncertainty of a factor of 2 within its current 3σ range. If an experiment is not background-free, a factor of two in effective mass corresponds to a combined factor of 16 improvement for the experimental parameters running time, detector mass, background level and energy resolution. Therefore, a more precise determination of θ_{12} is crucial for the interpretation of experimental results and the evaluation of the potential and requirements for future experiments. We give the required half-lives to exclude (and touch) the inverted hierarchy regime for all double beta decay isotopes with a Q -value above 2 MeV. The nuclear matrix elements from 6 different groups and, if available, their errors are used and compared. We carefully put the calculations on equal footing in what regards various convention issues. We also use our compilation of matrix elements to give the reachable values of the effective mass for a given half-life value.

*email: alexander.dueck@mpi-hd.mpg.de

†email: werner.rodejohann@mpi-hd.mpg.de

‡email: zuber@physik.tu-dresden.de

1 Introduction

Neutrinoless Double Beta Decay ($0\nu\beta\beta$) is a process of fundamental importance for particle physics [1–3]. In the best motivated interpretation [4] of this process, light Majorana neutrinos, whose mixing is observed in neutrino oscillation experiments, are exchanged in the process, and the particle physics quantity which is probed is the "effective mass"

$$\langle m_\nu \rangle = |U_{e1}^2 m_1 + U_{e2}^2 m_2 e^{i\alpha} + U_{e3}^2 m_3 e^{i\beta}|. \quad (1)$$

Here $U_{e1} = \cos\theta_{12} \cos\theta_{13}$, $U_{e2} = \sin\theta_{12} \cos\theta_{13}$ and $U_{e3}^2 = 1 - U_{e1}^2 - U_{e2}^2$. The current knowledge of these mixing angles is given in Table 1. The lifetime of $0\nu\beta\beta$ decay is inversely proportional to the effective mass squared.

Apart from verifying the Majorana nature of neutrinos, the effective mass depends on a number of known and unknown neutrino parameters, and testing or cross-checking the values of these parameters is obviously an immensely important task. Among the unknown neutrino parameters the neutrino mass ordering (the sign of the atmospheric mass-squared difference) is of particular interest. It is indeed an exciting possibility to rule out the inverted ordering (IH) with $0\nu\beta\beta$. This is possible because the lower limit of the effective mass is non-zero in this case [5, 6]. Actually, if at the time when the inverted hierarchy regime is under test at double beta decay experiments the mass ordering is known to be inverted (by an oscillation experiment or by a galactic supernova explosion), then testing the inverted hierarchy means testing directly the Majorana nature of neutrinos. If the mass ordering is not known, the experiments can rule out the inverted hierarchy only if in addition the Majorana nature of neutrinos is assumed. However, this happens in the vast majority of models and scenarios leading to neutrino mass, and is also natural from an effective field theory point of view.

In any case, a natural scale for the effective mass provided by particle physics is the minimal value of the effective mass in the inverted hierarchy, and should be the intermediate- or long-term aim of double beta experiments.

We stress in this paper that the lower limit of the effective mass is a sensitive function of the solar neutrino mixing angle θ_{12} : the current 3σ range of θ_{12} introduces an uncertainty of a factor of 2. In realistic, i.e. background dominated, experiments the achievable half-life reach is proportional to

$$T_{1/2}^{0\nu} \propto a \times \epsilon \times \sqrt{\frac{M \times t}{B \times \Delta E}}, \quad (2)$$

where a is the isotopical abundance of the double beta emitter, M the used mass, t the measuring time, ϵ the detection efficiency, ΔE the energy resolution at the peak position and B the background index typically given in counts/keV/kg/yr. Hence, an uncertainty of 2 in the effective mass corresponds to a factor of $2^2 = 4$ in terms of lifetime reach and a factor of $2^4 = 16$ uncertainty in the above combination of experimental parameters. In this work we aim to stress this fact and to illustrate its consequences. We quantify the requirements to test the inverted hierarchy in terms of necessary half-life reach. We consider all $0\nu\beta\beta$ -isotopes with a Q -value above 2 MeV and compile the nuclear matrix element

Parameter	Best-fit $^{+1\sigma}_{-1\sigma}$	3σ
$\sin^2 \theta_{12}$	$0.318^{+0.019}_{-0.016}$	0.27-0.38
$\sin^2 \theta_{13}$	$0.013^{+0.013}_{-0.009}$	≤ 0.053
Δm_{A}^2 [10^{-3} eV 2]	$2.40^{+0.12}_{-0.11}$	2.07-2.75
Δm_{O}^2 [10^{-5} eV 2]	$7.59^{+0.23}_{-0.18}$	7.03-8.27

Table 1: Neutrino mixing parameters: best-fit values as well as 1σ and 3σ ranges [7].

calculations from six different groups. That is, we study the isotopes ^{48}Ca , ^{76}Ge , ^{82}Se , ^{96}Zr , ^{100}Mo , ^{110}Pd , ^{116}Cd , ^{124}Sn , ^{130}Te , ^{136}Xe , and ^{150}Nd , as well as nuclear matrix element calculations applying QRPA [8, 9], Nuclear Shell Model [10], the Interacting Boson Model [11], the Generating Coordinate Method [12], and the projected-Hartree-Fock-Bogoliubov model [13]. Particular care is taken to put the calculations on equal footing in what regards various convention issues, such as the axial vector coupling g_A and the nuclear radius appearing in the phase space factor. We present the results for different values of θ_{12} , in order to show its impact.

We are taking the point of view that the spread of nuclear matrix elements and lifetimes obtained in our analysis is a fair estimate of the true allowed range. Though experimental approaches to reduce the uncertainty [14], and statistical approaches to better estimate the theoretical uncertainties (see e.g. [15]), have started, at the current stage the collection of available results and the use of their spread is the most pragmatic procedure.

Nevertheless, our main conclusions are independent of this and quite straightforward: a precision determination of the solar neutrino mixing angle is crucial to determine the physics potential of, and requirements for, neutrinoless double beta decay experiments. Some proposals for solar neutrino experiments which can pin down θ_{12} more precisely can be found in the literature [16–19]. Large-scale long baseline reactor neutrino experiments have also been proposed [20–23], but to our knowledge still await detailed study by experimentalists. The main focus of future precision neutrino oscillation physics is put on mass ordering, the other mixing angles and CP violation in facilities such as super-, beta-beams or neutrino factories. Given the impact of θ_{12} on neutrinoless double beta decay that we discuss here, we hope to provide additional motivation for studies and proposals in order to determine θ_{12} as precisely as possible¹. At least we encourage to seriously determine and optimize the potential of future experiments in what regards the achievable precision of θ_{12} .

Using our compilation of matrix element calculations, we also present results for the

¹The additional physics potential of precision solar neutrino or θ_{12} experiments is e.g. solving the metallicity problem of the Sun [24], probing the transition region of the electron neutrino survival probability in the Sun’s interior [25], or distinguishing theoretical approaches to lepton mixing such as tri-bimaximal mixing from alternative models [26].

$\sin^2 \theta_{12}$	$\langle m_\nu \rangle_{\min}^{\text{IH}} [\text{eV}]$	
	minimal	maximal
0.270	0.0196	0.0240
0.318	0.0154	0.0189
0.380	0.0100	0.0123

Table 2: Lower limit of the effective electron neutrino mass in the case of an inverted hierarchy for different values of $\sin^2 \theta_{12}$. The minimal and maximal values are obtained by varying Δm_{A}^2 , Δm_{C}^2 and $\sin^2 \theta_{13}$ in their allowed 3σ ranges.

necessary half-life in order to touch the inverted hierarchy regime. Finally, we investigate which limits on the effective mass can be achieved for a given half-life, and what the current limits are. These points are independent of the value of θ_{12} .

We find that the isotope ^{100}Mo tends to be interesting, in the sense that with the same lifetime it can slightly more easily rule out the inverted hierarchy, or achieve the better limit on the effective mass. This may be helpful for experiments considering various alternative isotopes to study.

The paper is built up as follows: in Section 2 we shortly discuss the effective mass and its dependence on the solar neutrino mixing angle in the inverted hierarchy. Section 3 deals with the various calculations of the nuclear matrix elements and their impact on ruling out and touching the inverted hierarchy regime. We point out the difficulties arising from the chosen convention, which can arise by comparing different nuclear matrix element calculations. The general limits on the effective mass as a function of an achievable half-life are given in a short Section 3.3, where also current limits on the effective mass are compiled. In Section 4 we give some examples on the experimental consequences of our results for future experiments. Tables and details are delegated to the Appendices, and conclusions are presented in Section 5.

2 Effective neutrino mass and experimental values of neutrino oscillation parameters

In general, the decay rate of $0\nu\beta\beta$ decay factorizes in a kinematical, nuclear physics and particle physics part:

$$\Gamma^{0\nu} = G_{\text{kin}} |M_{\text{nucl}}|^2 X_{\text{part}}. \quad (3)$$

The observation of the decay would establish the nature of the neutrino as a Majorana particle [27], independent on whether indeed light Majorana neutrinos are exchanged in the diagram leading to $0\nu\beta\beta$. However, the most natural interpretation is indeed that this is the case, because we know that neutrinos have a non-vanishing rest mass, and in the vast majority of models they are Majorana particles. The particle physics parameter in

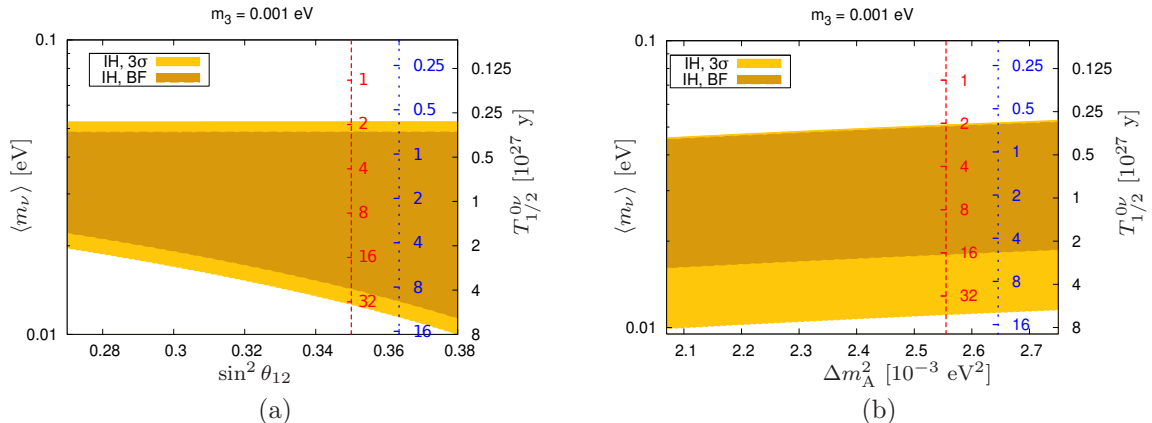


Figure 1: The effective electron neutrino mass in the case of an inverted hierarchy is shown as a function of (a) $\sin^2 \theta_{12}$ and (b) Δm_A^2 with best-fit values and 3σ ranges for the other oscillation parameters. On the right side of the plots the corresponding half-life for ^{76}Ge is shown assuming three different nuclear matrix elements: $M^{0\nu} = 2.81$ (red dashed axis), $M^{0\nu} = 5$ (blue dotted axis), and $M^{0\nu} = 7.24$ (black solid axis).

the decay width Eq. (3) is therefore $X_{\text{part}} \propto \langle m_\nu \rangle^2$, where $\langle m_\nu \rangle$ is the effective electron neutrino mass defined as

$$\langle m_\nu \rangle = \left| c_{12}^2 c_{13}^2 m_1 + s_{12}^2 c_{13}^2 m_2 e^{i\alpha} + s_{13}^2 m_3 e^{i\beta} \right|, \quad (4)$$

where $c_{ij} = \cos \theta_{ij}$, $s_{ij} = \sin \theta_{ij}$, and α, β are the two Majorana phases. It depends on the three neutrino mass eigenstates m_i and the first row of the Pontecorvo-Maki-Nakagawa-Sakata (PMNS) mixing matrix. The effective mass, $\langle m_\nu \rangle$, can span a wide range due to the unknown Majorana phases, the unknown total neutrino mass scale, and the unknown mass ordering. We are interested here mostly in the case of the inverted hierarchy (IH), which corresponds to $m_2 > m_1 > m_3$. In this case the maximum and minimum values of $\langle m_\nu \rangle$ are given by (see e.g., [5, 6, 28])

$$\langle m_\nu \rangle_{\text{max}}^{\text{IH}} = \sqrt{m_3^2 + \Delta m_A^2 c_{12}^2 c_{13}^2} + \sqrt{m_3^2 + \Delta m_\odot^2 + \Delta m_A^2 s_{12}^2 c_{13}^2} + m_3 s_{13}^2, \quad (5)$$

and

$$\langle m_\nu \rangle_{\text{min}}^{\text{IH}} = \sqrt{m_3^2 + \Delta m_A^2 c_{12}^2 c_{13}^2} - \sqrt{m_3^2 + \Delta m_\odot^2 + \Delta m_A^2 s_{12}^2 c_{13}^2} - m_3 s_{13}^2, \quad (6)$$

respectively. Here, $\Delta m_\odot^2 = m_2^2 - m_1^2$ is the solar and $\Delta m_A^2 = |m_3^2 - m_1^2|$ the atmospheric mass-squared difference. The values we use for the mixing parameters are shown in Table 1.

Unless the smallest mass m_3 is larger than about 0.05 eV, the effective mass does basically not depend on its value, and increases linearly with m_3 afterwards. In the case of $m_3 \lesssim 0.05$ eV, one finds

$$\langle m_\nu \rangle_{\text{max}}^{\text{IH}} \simeq c_{13}^2 \sqrt{\Delta m_A^2}, \quad (7)$$

and

$$\langle m_\nu \rangle_{\min}^{\text{IH}} \simeq c_{13}^2 \sqrt{\Delta m_A^2} \cos 2\theta_{12} = (1 - |U_{e3}|^2) \sqrt{\Delta m_A^2} (1 - 2 \sin^2 \theta_{12}), \quad (8)$$

respectively. The maximal value is obtained for $\alpha = 0$ and the minimal value for $\alpha = \pi/2$. Since θ_{12} is non-maximal, the minimal value of $\langle m_\nu \rangle$ is non-zero, which is in contrast to the normal mass ordering, in which the effective mass can vanish. By obtaining experimentally an upper limit on the effective mass below $\langle m_\nu \rangle_{\min}^{\text{IH}}$, we can rule out the inverted ordering. If we would know by independent evidence that the ordering is inverted (i.e., from a long baseline experiment, or observation of a galactic supernova), then obtaining such an upper limit would even mean that the Majorana nature of neutrinos would have been ruled out.

From a more pragmatic point of view, particle physics provides a scale for limits on the effective mass, which should be the sensitivity goals of the experimental program. These values are $\langle m_\nu \rangle_{\max}^{\text{IH}}$ and $\langle m_\nu \rangle_{\min}^{\text{IH}}$ given in Eq. (7) and (8), respectively. In Fig. 1 we show the effective mass for the best-fit and the 3σ ranges of the oscillation parameters as a function of $\sin^2 \theta_{12}$ and Δm_A^2 . It is clear that the dependence of the lower limit on $\sin^2 \theta_{12}$ is very strong. In the currently allowed 3σ range the range of θ_{12} quantifies to a factor of 2 uncertainty for $\langle m_\nu \rangle_{\min}^{\text{IH}}$, which translates into a factor $2^2 = 4$ in lifetime reach for an experiment. We illustrate this in the plots by translating $\langle m_\nu \rangle$ into the half-life for ^{76}Ge for three representative values of the nuclear matrix elements (see Section 3.1). Table 2 shows the numerical values of the effective electron neutrino mass in the case of an inverted hierarchy for different values of the solar neutrino parameter $\sin^2 \theta_{12}$. The uncertainty in the other parameters $|U_{e3}|$ and Δm_A^2 is by far not as significant, it amounts in total to a factor less than 25 %. An extensive program to test Δm_A^2 and $|U_{e3}|$ is underway (see e.g. [29]) and will have decreased this uncertainty considerably by the time the $0\nu\beta\beta$ -experiments of the required sensitivity are running. The maximal value of the effective mass does not depend on θ_{12} , and hence its value is uncertain by less than 25 %.

3 Half-life sensitivities and the inverted hierarchy

We have seen above that in order to rule out the inverted ordering, and to evaluate the physics potential of future experiments, the value of θ_{12} is of crucial importance. We will now attempt to quantify the impact of θ_{12} in terms of experimentally required half-life. Towards this end, we will have to care with the available calculations of the nuclear matrix elements (NMEs). We have scanned the literature and extracted the NME values for five different calculational approaches of six different groups. If given by the respective authors, we include the error estimates in the calculations for our results. In order to compare them in a proper way, we carefully try to put the NMEs on equal footing, because details of conventions are often different in different publications. We then consider all 11 potential $0\nu\beta\beta$ -isotopes with a Q -value above 2 MeV. We discuss the necessary half-lives to rule out and to touch the inverted hierarchy, putting particular emphasis on the θ_{12} -dependence if necessary. Finally, using our compilation we also give the limits on $\langle m_\nu \rangle$ as a function of future half-life limits for the 11 interesting isotopes. Using the published half-life limits of

Isotope	$G^{0\nu}$ [10^{-14} yrs $^{-1}$]	Q [keV]	nat. abund. [%]
^{48}Ca	6.35	4273.7	0.187
^{76}Ge	0.623	2039.1	7.8
^{82}Se	2.70	2995.5	9.2
^{96}Zr	5.63	3347.7	2.8
^{100}Mo	4.36	3035.0	9.6
^{110}Pd	1.40	2004.0	11.8
^{116}Cd	4.62	2809.1	7.6
^{124}Sn	2.55	2287.7	5.6
^{130}Te	4.09	2530.3	34.5
^{136}Xe	4.31	2461.9	8.9
^{150}Nd	19.2	3367.3	5.6

Table 3: $G^{0\nu}$ for different isotopes using $r_0 = 1.2$ fm. Values taken from Table 6 of Ref. [9] ($G_1^{0\nu}$ in their notation) and scaled to $g_A = 1.25$ ($G^{0\nu}$ of ^{110}Pd taken from Table IV of Ref. [13]). Also shown is the Q -value for the ground-state-to-ground-state transition which is calculated using isotope masses from Ref. [30] and the natural abundance in percent. Note that there is a misprint in Ref. [9], which quotes $G^{0\nu}$ for ^{100}Mo as 11.3×10^{-14} yrs $^{-1}$.

different isotopes, we also give the current limits on the effective mass.

3.1 Nuclear Matrix Elements and the Half-life

The $0\nu\beta\beta$ decay half-life is given according to Eq. (3) by² [31]

$$(T_{1/2}^{0\nu})^{-1} = G^{0\nu} |M^{0\nu}|^2 \left(\frac{\langle m_\nu \rangle}{m_e} \right)^2, \quad (9)$$

where $G^{0\nu}$ is the phase space factor, $M^{0\nu}$ the NME, m_e the electron mass, and the effective electron neutrino mass $\langle m_\nu \rangle$ as given in Eq. (4). It is known that the conversion of a lifetime into an effective mass, in particular when different NMEs are compared, should be performed carefully [32, 33]. The nuclear physics parameters, for instance the axial-vector coupling g_A lying in the range $1 \lesssim g_A \lesssim 1.25$, should strictly speaking introduce an uncertainty in the value of $M^{0\nu}$ only. However, it is convention to include g_A in the phase space factor as well. In addition, the nuclear radius $R_A = r_0 A^{1/3}$ (A being the atomic number) appears in $G^{0\nu}$, and there are differences in the normalization of R_A with r_0 , which should be taken into account. This leads to the small complication that NMEs calculated with different values for g_A and r_0 cannot be directly compared with each other, since they have different phase space factors and hence seemingly equal (by their value) matrix elements will lead to different decay half-lives [32] (see also the Appendix of [34]). We will outline these issues in more detail in what follows.

²Note that sometimes the factor $1/m_e^2$ is carried into the definition of $G^{0\nu}$.

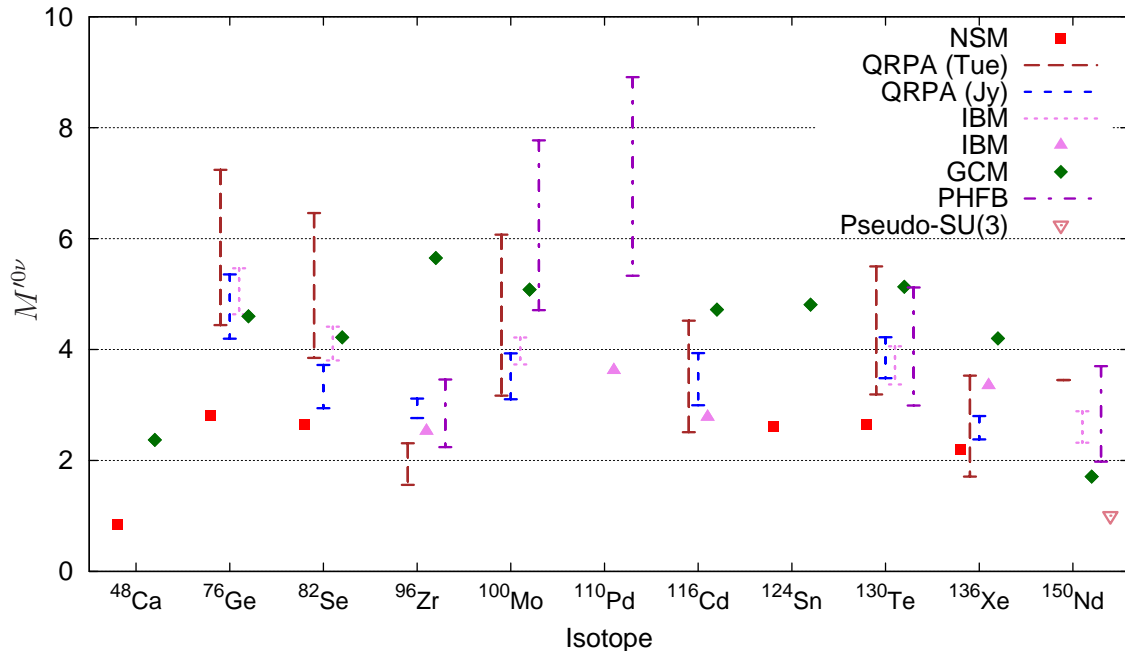


Figure 2: NMEs calculated in different frameworks. We have scaled the cited values to $r_0 = 1.2$ fm and $g_A = 1.25$ (see Eq. (11)) to make them directly comparable. The exact values are given in Table 4.

The phase space factor is through convention proportional to g_A^4/R_A^2 [9],

$$G^{0\nu} \propto \frac{g_A^4}{R_A^2}, \quad (10)$$

with $R_A = r_0 A^{1/3}$ being the nuclear radius and $1 \lesssim g_A \lesssim 1.25$ the axial-vector coupling. The dependence on R_A stems from the desire to make the NMEs dimensionless. Therefore in the definition of the NMEs there is a factor of R_A which is compensated for by the factor $1/R_A^2$ in $G^{0\nu}$. To resolve the issue of comparing matrix elements calculated using different values of g_A , some – but not all – authors define

$$M'^{0\nu} = \left(\frac{g_A}{1.25} \right)^2 M^{0\nu}, \quad (11)$$

thereby carrying the g_A dependence from $G^{0\nu}$ to $M'^{0\nu}$, i.e.,

$$G^{0\nu} (M'^{0\nu})^2 = G_{1.25}^{0\nu} (M^{0\nu})^2, \quad (12)$$

with $G_{1.25}^{0\nu} = G^{0\nu}(g_A = 1.25)$. This means that these NMEs share a common $G^{0\nu}$ factor – that of $g_A = 1.25$. Still one has to be careful when comparing NMEs from different groups, since different authors take different values for r_0 , usually $r_0 = 1.1$ fm (e.g. Ref. [35, 36]) or

Isotope	NSM [10] (UCOM)	Tü [35,36] (CCM)	Jy [37] (UCOM)	IBM [11] (Jastrow)	GCM [12] (UCOM)	PHFB [13] (mixed)
⁴⁸ Ca	0.85	-	-	-	2.37	-
⁷⁶ Ge	2.81	4.44 - 7.24	4.195 - 5.355	4.636 - 5.465	4.6	-
⁸² Se	2.64	3.85 - 6.46	2.942 - 3.722	3.805 - 4.412	4.22	-
⁹⁶ Zr	-	1.56 - 2.31	2.764 - 3.117	2.530	5.65	2.24 - 3.46
¹⁰⁰ Mo	-	3.17 - 6.07	3.103 - 3.931	3.732 - 4.217	5.08	4.71 - 7.77
¹¹⁰ Pd	-	-	-	3.623	-	5.33 - 8.91
¹¹⁶ Cd	-	2.51 - 4.52	2.996 - 3.935	2.782	4.72	-
¹²⁴ Sn	2.62	-	-	-	4.81	-
¹³⁰ Te	2.65	3.19 - 5.50	3.483 - 4.221	3.372 - 4.059	5.13	2.99 - 5.12
¹³⁶ Xe	2.19	1.71 - 3.53	2.38 - 2.802	3.352	4.2	-
¹⁵⁰ Nd	-	3.45	-	2.321 - 2.888	1.71	1.98 - 3.7

Table 4: NMEs calculated in different frameworks. The method used to take into account short-range correlations is indicated in brackets. We have scaled the cited values to $r_0 = 1.2$ fm and $g_A = 1.25$ (see Eq. (11)) to make them directly comparable. If ranges instead of single NME values are given then they arise due to intrinsic model details varied in the respective publications. This table is graphically represented in Fig. 2, the pseudo-SU(3) NME for ¹⁵⁰Nd plotted there is 1.00 [38].

$r_0 = 1.2$ fm (e.g. Ref. [10, 11, 37]). The NMEs are proportional to r_0 and therefore when comparing two different matrix elements $M_1^{0\nu}$, $M_2^{0\nu}$, which have been calculated using $r_{0,1}$ and $r_{0,2}$, respectively, one has to rescale $M_2^{0\nu}$ by $r_{0,1}/r_{0,2}$ or $M_1^{0\nu}$ by $r_{0,2}/r_{0,1}$. Otherwise one introduces an error of $(r_{0,1}/r_{0,2})^2 \simeq 1.19$ in terms of half-life (see Eq. (9)). A compilation of g_A , r_0 and $G^{0\nu}$ values used in different works can be found in Ref. [33].

In addition, it is often overlooked that there are differences between independent phase space factor calculations, which can be as high as $\sim 13\%$ (see the Appendix of [34]). For instance, Ref. [35] uses phase space factors from [39], while Ref. [37] uses the ones from [9]. There, $G^{0\nu}$ for the isotope ¹³⁶Xe is given as $49.7 \times 10^{-15} \text{ yrs}^{-1}$ and $43.1 \times 10^{-15} \text{ yrs}^{-1}$, respectively (we scaled them to $g_A = 1.25$ and $r_0 = 1.2$ fm to make them directly comparable). To perform a consistent comparison between different NME calculations we will take the numerical values for the phase space factors from Ref. [9] when calculating the necessary half-life sensitivities and take carefully into account all of the above mentioned difficulties³. Table 3 shows the phase space factors used in our calculations. All $0\nu\beta\beta$ -isotopes with a Q -value above 2 MeV are given. We have chosen the value $r_0 = 1.2$ fm throughout our analysis. Also given in the table is the natural abundance of the isotope in percent.

The convention issues mentioned so far are of course different from the intrinsic uncertainty stemming from the nuclear physics itself. We will not get into detail here, and refer to existing reviews available in the literature [1, 9]. A program to reduce the uncertainty

³Note that there is a misprint for the phase space factor of ¹⁰⁰Mo in Ref. [9].

by independent experimental cross checks has been launched [14], but it is unclear whether the results will be available and conclusive for all interesting isotopes at the time when the decisions on the experimental parameters have to be taken.

An important point here are short-range correlations (SRC) since the contribution to NMEs stems mainly from physics of internucleon distances $r \leq (2 - 3)$ fm [40]. There are different proposals how to treat SRC, namely via a Jastrow-like function [1, 41], Unitary Correlation Operator Method (UCOM) [42], or Coupled Cluster Method (CCM) [35, 43–45]. For instance, the authors of Ref. [37] argue that UCOM should be preferred over Jastrow while the authors of [35] prefer CCM. In this work we use the NME values calculated with UCOM or CCM SRC in the NSM, QRPA, and GCM frameworks; the NME values in the IBM framework are calculated with Jastrow SRC. In the case of the PHFB model the authors used a statistical estimate of the theoretical uncertainty by calculating NMEs with three different types of SRC, four different parametrizations of the effective two-body interaction and taking the mean and the standard deviation. We used the NMEs derived in this manner and therefore no particular SRC method can be assigned to them. With a chosen SRC method, some groups discuss additional sources of error which arise, such as the set of single-particle states, the number of possible wave function configurations, or other model details. These errors are given in some publications, and we include them in our analysis. The NME values and ranges we have compiled and will be used in this work are tabulated in Table 4 and plotted in Fig. 2. The values are scaled to $r_0 = 1.2$ fm and $g_A = 1.25$ so that they are directly comparable. The original NME values can be found in column 3 of Table 8 of Ref. [10] (NSM), column 6 of Table III of Ref. [35] and column 4 of Table II of Ref. [36] (QRPA, Tübingen group), column 6 of Table 1 of Ref. [37] (QRPA, Jyväskylä group), columns 2 and 3 of Table VI of Ref. [11] (IBM), column 5 of Table I of Ref. [12] (GCM), and column 3 of Table IV of Ref. [13] (PHFB). Regarding IBM, the isotopes for which a range is given are calculated in Ref. [11] with two sets of single-particle energies, one extracted from experiment (“experimental”), the other from a specific model (“theoretical”). Their span defines the given range. The IBM values without a range are unpublished “experimental” NMEs kindly provided by Francesco Iachello. As only few calculations for ^{150}Nd are available, we also include the result from Ref. [38], which applied the pseudo-SU(3) Ansatz for the calculation, which is suitable for deformed nuclei such as ^{150}Nd . It gives by far the lowest NME.

3.2 Ruling out the inverted hierarchy

Having compiled the NMEs in a form which makes it possible to compare them with each other, we can now give the necessary half-lives in order to rule out the inverted hierarchy. Recall that the value $\langle m_\nu \rangle_{\min}^{\text{IH}}$ given in Eq. (8) has to be reached for this, and that a strong dependence on θ_{12} is present.

In Fig. 3 we plot the necessary half-lives to rule out the inverted hierarchy for all 11 isotopes with Q -value above 2 MeV. We display the situation for different values of θ_{12} , which correspond to the best-fit value of the current oscillation analyses, and the lower and upper limit of the current 3σ range. The full range, leaving θ_{12} free within its current range,

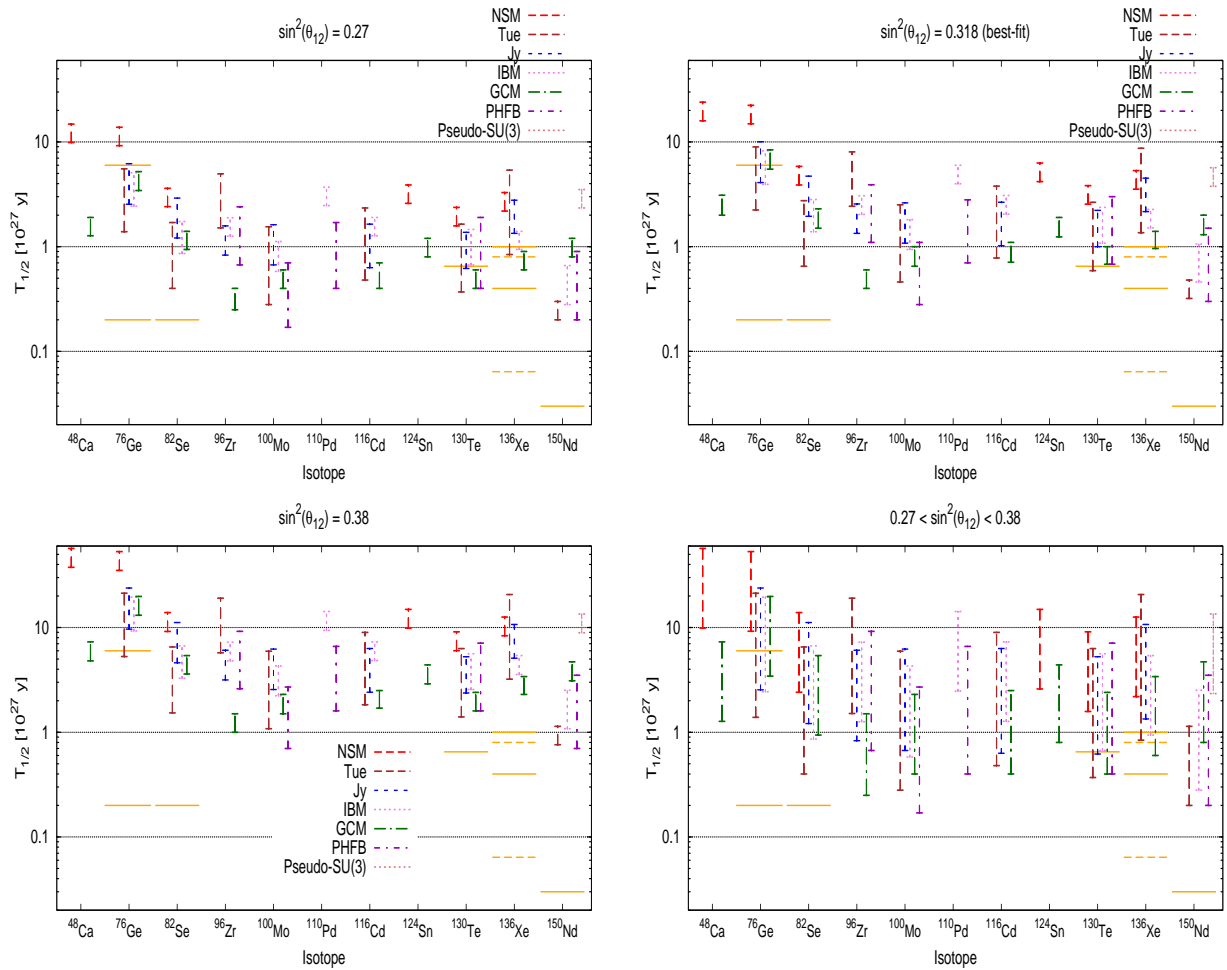


Figure 3: Required half-life sensitivities to exclude the inverted hierarchy for different values of θ_{12} . For each value of $\sin^2 \theta_{12}$ the other parameters (Δm_A^2 , Δm_\odot^2 , $\sin^2 \theta_{13}$) are varied in their 3σ ranges. The lower right plot tries to combine the other three: the lines correspond to the combined uncertainties of the nuclear physics and the oscillation parameters. The small horizontal lines show expected half-life sensitivities at 90% C.L. of running and planned $0\nu\beta\beta$ experiments. The expected limits are from the following experiments: GERDA and MAJORANA (^{76}Ge , equal sensitivity expectations for both experiments); SuperNEMO (^{82}Se), CUORE (^{130}Te); EXO (^{136}Xe , dashed lines); KamLAND (^{136}Xe , solid lines); SNO+ (^{150}Nd). When two sensitivity expectations are given for one experiment they correspond to near and far time goals.

is also displayed. For convenience, we give the numerical values for necessary $T_{1/2}^{0\nu}$ in Table 7, which can be found in the Appendix. For each value of $\sin^2 \theta_{12}$ the other parameters (Δm_A^2 , Δm_\odot^2 , $\sin^2 \theta_{13}$) are varied in their 3σ ranges such that in Table 7 one has a somewhat more optimistic and more pessimistic prediction for the $0\nu\beta\beta$ decay half-life. Recall that

Isotope	Experiment	$T_{1/2}^{0\nu}/\text{yrs}$
^{76}Ge	GERDA	2.0×10^{26}
	(+MAJORANA)	6.0×10^{27}
^{82}Se	SuperNEMO	2.0×10^{26}
^{130}Te	CUORE	6.5×10^{26}
^{136}Xe	EXO	6.4×10^{25}
		8.0×10^{26}
^{136}Xe	KamLAND	4.0×10^{26}
		1.0×10^{27}
^{150}Nd	SNO+	4.5×10^{24}
		3.0×10^{25}

Table 5: Expected half-life sensitivities for some $0\nu\beta\beta$ experiments [46]. When two values are given they correspond to near and far time expectations with different detector masses.

the dependence on the oscillation parameters other than θ_{12} is rather weak (less than 25 %) and will be strongly reduced in the future.

One can compare the necessary half-lives with the foreseen sensitivities of up-coming experiments. We refer here to the compilation from Ref. [46], which listed confirmed sensitivities of the currently “most developed” experiments. Table 5 gives the numbers, staged experiments have two values. We have included those sensitivities in our plots. To give an example on the interpretation of the plots, with the final sensitivity GERDA and Majorana (6×10^{27} yrs) could rule out the inverted hierarchy if $\sin^2 \theta_{12} = 0.27$ for all NMEs except for the NSM.

Another way to display the interplay of nuclear physics, θ_{12} and $0\nu\beta\beta$ is shown in Fig. 4: assuming for four interesting isotopes a certain half-life limit, we show for which NME values the inverted hierarchy is ruled out. For instance, for ^{76}Ge and a half-life of 5×10^{27} yrs, we can rule out the inverted hierarchy if the matrix element is larger than about 5 if $\sin^2 \theta_{12} = 0.32$. For a half-life of 1×10^{27} yrs, the NME has to be larger than about 12, hence not too realistic. Nevertheless, the ranges of the NME calculations are also displayed in the figures.

Fig. 5 shows the required half-life to touch the inverted hierarchy. This half-life (corresponding to the value $\langle m_\nu \rangle_{\text{max}}^{\text{IH}}$ given in Eq. (7)) does not depend on θ_{12} . The other parameters, Δm_{A}^2 , Δm_{C}^2 and θ_{13} are varied in their current 3σ range. The numerical values are given in Table 8. For instance, the combined GERDA and Majorana results, as well as CUORE, could touch the inverted hierarchy for all available NMEs.

From the figures and tables presented in this Section, one identifies ^{100}Mo as the somewhat most interesting isotope. With our compilation of NMEs, the required lifetimes to reach and/or exclude the inverted hierarchy tends to be generally lowest for this $0\nu\beta\beta$ -candidate. If the very low pseudo-SU(3) NME for ^{150}Nd would be omitted, then this isotope would even more favorable than ^{100}Mo . These tentative conclusions may be helpful for experiments

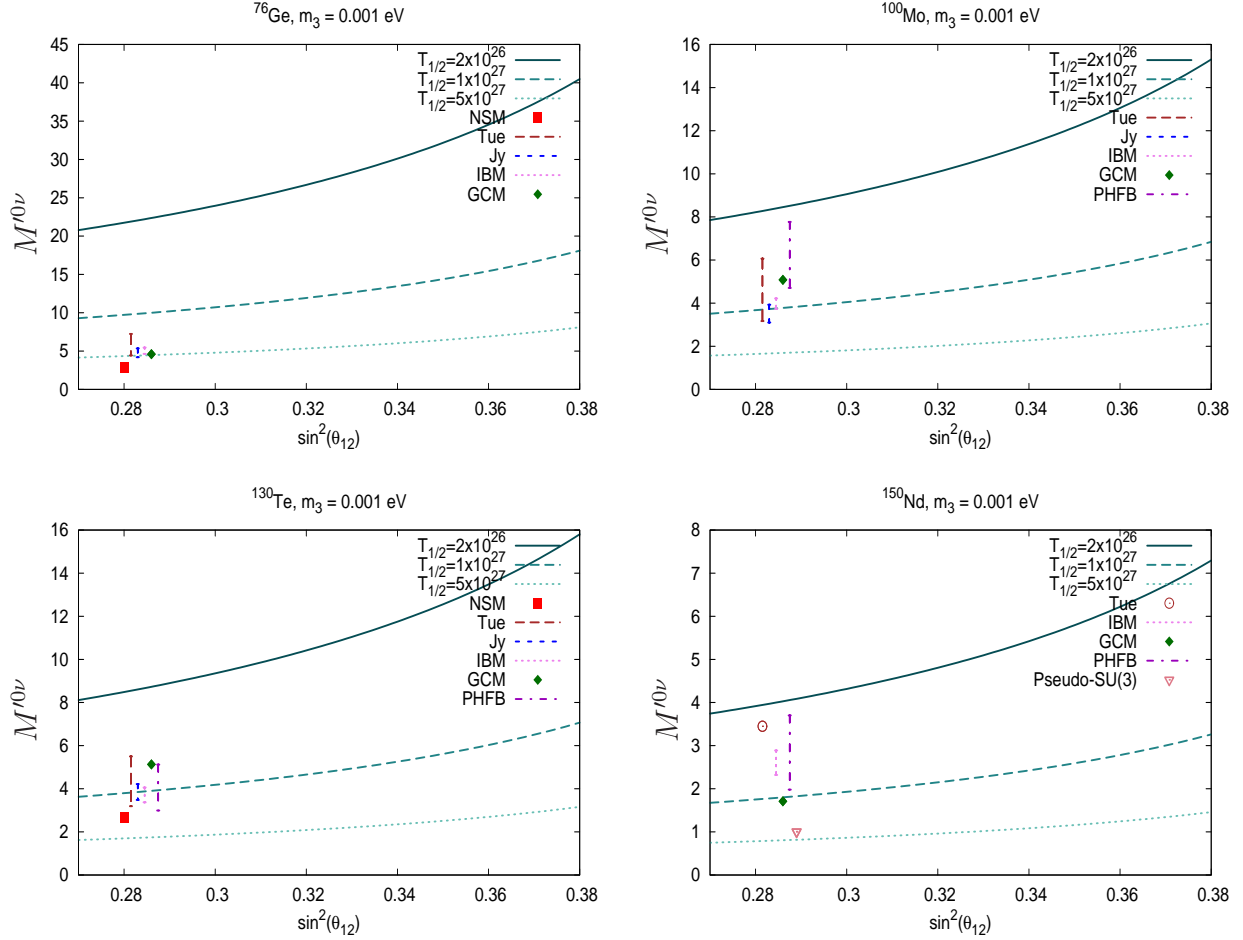


Figure 4: Assuming the case of an inverted neutrino mass hierarchy and a measurement of a $0\nu\beta\beta$ decay signal, this plot shows the minimal NMEs for which the inverted hierarchy can be ruled out. For the mixing parameters Δm_{Λ}^2 , Δm_{\odot}^2 , and $\sin^2 \theta_{13}$ best-fit values are taken. The ranges of the NME calculations are also displayed in the figures.

which have alternatives in the isotopes to investigate, such as LUCIFER [47] (currently considering ^{82}Se or ^{100}Mo or ^{116}Cd), MOON [48] (^{82}Se or ^{100}Mo), or SuperNEMO [49] (^{82}Se , ^{150}Nd or others).

3.3 Current and future limits on the effective mass

In Table 6 we show the current limits on the half-life of $0\nu\beta\beta$, obtained in a variety of experiments⁴. Using the largest and smallest NME from our compilation, we give the

⁴Part of the Heidelberg-Moscow collaboration has claimed observation [59] of $0\nu\beta\beta$ corresponding to a half-life of 2.23×10^{25} yrs, and a 95% C.L. range of $(0.8 - 18.3) \times 10^{25}$ yrs. This would correspond to a

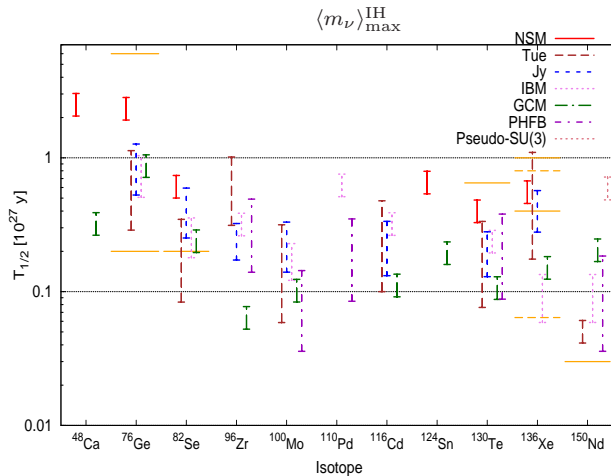


Figure 5: Required half-life sensitivities to touch the inverted hierarchy. The mixing parameters are varied in their 3σ ranges. The small horizontal lines show expected half-life sensitivities as in Fig. 3.

range of the current limit of $\langle m_\nu \rangle$ for the particular isotope.

Finally, we give the limit on the effective mass as a function of achieved half-life for the 11 isotopes under investigation. This is shown in Fig. 6. We have given four different half-life values. With a half-life sensitivities of about 5×10^{25} yrs the first isotopes start to touch the inverted hierarchy. Without specifying the value of θ_{12} , no isotope can rule out the inverted hierarchy unless sensitivities above 10^{27} yrs are reached. Entering the inverted hierarchy regime requires sensitivities above 10^{26} yrs.

4 Experimental consideration

A large variety of different upcoming experiments exists in various stages of realization. They are in order of increasing isotope mass CANDLES [60] (^{48}Ca), GERDA [61] and MAJORANA [62] (^{76}Ge), LUCIFER [47] (^{82}Se or ^{100}Mo or ^{116}Cd), SuperNEMO [49] (^{82}Se or ^{150}Nd), MOON [48] (^{82}Se or ^{100}Mo), COBRA [63] (^{116}Cd), CUORE [64] (^{130}Te), EXO [65], XMASS [66], KamLAND-Zen [67] and NEXT [68] (^{136}Xe), DCBA [69] and SNO+ [70] (^{150}Nd). As discussed before not for all proposals the final decision on the selected isotope is already made. From the discussion of the previous sections it would of course be desirable to rule out the inverted scenario and thus tune the experimental parameters and hence the sensitivity to do so. The obtainable half-life can be estimated to be

$$T_{1/2}^{0\nu} = \frac{N_A \ln 2}{n_\sigma} \left(\frac{a \times \epsilon}{W} \right) M \times t \quad (13)$$

range of the effective mass of (0.19 – 0.49) eV, and (0.066 – 0.82) eV, respectively.

Isotope	$T_{1/2}^{0\nu}/\text{yrs}$	Experiment	$M^{0\nu}$		$\langle m_\nu \rangle$ [eV]	
			min	max	min	max
^{48}Ca	5.8×10^{22}	CANDLES [50]	0.85	2.37	3.55	9.91
^{76}Ge	1.9×10^{25}	HDM [51]	2.81	7.24	0.21	0.53
^{82}Se	3.2×10^{23}	NEMO-3 [52]	2.64	6.46	0.85	2.08
^{96}Zr	9.2×10^{21}	NEMO-3 [53]	1.56	5.65	3.97	14.39
^{100}Mo	1.0×10^{24}	NEMO-3 [52]	3.10	7.77	0.31	0.79
^{116}Cd	1.7×10^{23}	SOLOTVINO [54]	2.51	4.72	1.22	2.30
^{130}Te	2.8×10^{24}	CUORICINO [55]	2.65	5.50	0.27	0.57
^{136}Xe	5.0×10^{23}	DAMA [56]	1.71	4.20	0.83	2.04
^{150}Nd	1.8×10^{22}	NEMO-3 [57]	1.71	3.70	2.35	8.65

Table 6: Experimental $0\nu\beta\beta$ decay half-life limits at 90 % C.L. Columns 4 and 5 show the minimal and maximal NMEs from our compilation (see Table 4), and columns 6 and 7 the corresponding upper limits on the effective electron neutrino mass $\langle m_\nu \rangle$. Similar limits on ^{76}Ge to the ones in [51] have been obtained by the IGEX experiment [58].

in a background-free scenario and

$$T_{1/2}^{0\nu} = \frac{N_A \ln 2}{n_\sigma} \left(\frac{a \times \epsilon}{W} \right) \sqrt{\frac{M \times t}{B \times \Delta E}} \quad (14)$$

in case of a background limited search [3], where n_σ is the number of standard deviations corresponding to the desired confidence level, W the molecular weight of the source material, and the other parameters as in Eq. (2). Notice, only in the background-free scenario the half-life sensitivity scales linearly with the measuring time. To be more conservative and realistic we assume a background limited case. As shown in Fig. 1a, the minimal effective Majorana mass which has to be explored shows a factor of two difference due to the current uncertainty in the mixing angle θ_{12} , depending on whether the actual value of θ_{12} comes off at the high or low end of its currently allowed range. Thus, this implies a factor of 16 difference in the combination of measuring time, energy resolution, background index and detector mass. From the experimental point of view such a big potential factor causes a significant challenge and work, as half-life measurements well beyond 10^{26} yrs itself are already non-trivial. Therefore it would be extremely desirable to reduce the uncertainty on θ_{12} in future solar experiments like SNO+.

As an example consider a 1 ton Ge-experiment, enriched to 90 % in ^{76}Ge . Furthermore, consider a full detection efficiency, an energy resolution (FWHM) of 3 keV at peak position, the best one of all considered double beta experiments, and 10 years of running time. For an optimistic combination of the other mixing parameters (upper rows in Tables 7 and 8) such an experiment could touch the IH at 2σ C.L. even using the less favorable NME if a background level of 5.5×10^{-3} counts/keV/kg/yr could be achieved. This should be feasible as already for GERDA phase II the aim is to achieve 10^{-3} counts/keV/kg/yr. Ruling out

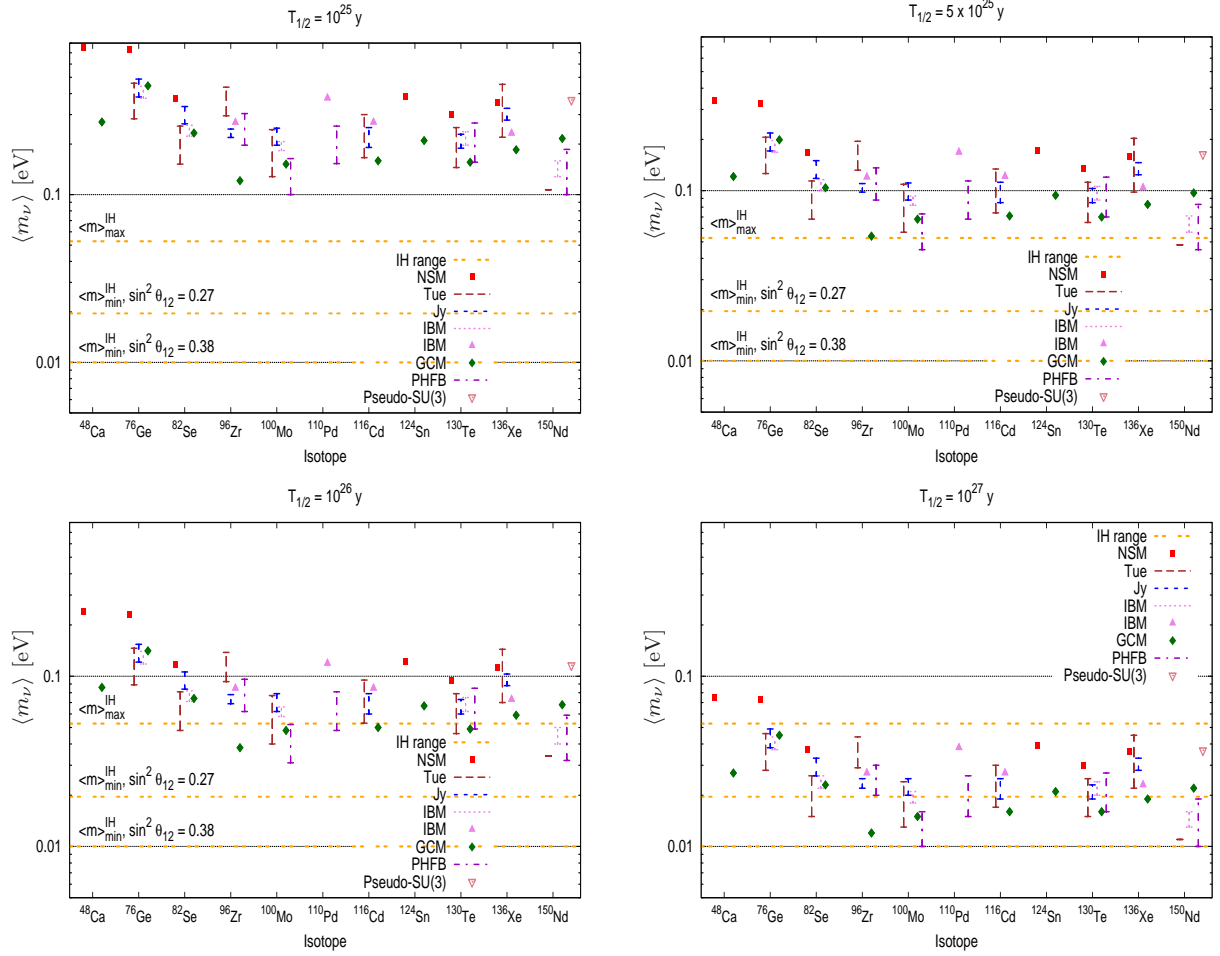


Figure 6: Limits on the effective mass which can be set assuming different half-lives for the 11 isotopes under investigation. The orange double-dashed horizontal lines show the upper and lower lines of the inverted hierarchy when the mixing parameters are varied in their 3σ range (see Fig. 1). Thereby the horizontal line at 0.02 eV (0.01 eV) corresponds to the lower line of the IH for $\sin^2 \theta_{12} = 0.27$ ($\sin^2 \theta_{12} = 0.38$).

the complete IH for small θ_{12} would require 2.4×10^{-4} counts/keV/kg/yr. For large θ_{12} it is not possible to exclude the IH (assuming the smallest NME) with the considered experimental parameters. Excluding the IH would require a half-life sensitivity of 3.5×10^{28} yrs (Tab. 7). But even considering a background-free case and therefore using Eq. (13), one obtains a 2σ half-life limit of only 2.47×10^{28} yrs. By using Eq. (14) one could formally calculate a necessary background of 1.6×10^{-5} counts/keV/kg/yr to exclude a half-life of 3.5×10^{28} yrs with the stated experimental set-up. But this background corresponds to only about 0.5 total background counts during the whole operational period of 10 years which has to be compared to 1.4 expected counts from the $0\nu\beta\beta$ decay with a half-life of

3.5×10^{28} yrs. Hence, the experiment cannot be considered to be background dominated and thus Eq. (14) is not applicable.

As another example, consider a large scale experiment like SNO+ using ^{150}Nd , enriched to 60%. With a total mass of 760 kg of natural Nd, 10 years of running time and an energy resolution of about 300 keV (the resolution depends on the percentage of Nd-loading of the scintillator, here a resolution of $3.5\%/\sqrt{E}$ was assumed) it would require a background of 6.1×10^{-4} counts/keV/kg/yr to touch the IH at 2σ C.L. To exclude IH a background as small as 2.7×10^{-5} counts/keV/kg/yr (for small θ_{12}) or 1.9×10^{-6} counts/keV/kg/yr (for large θ_{12}) would be required (note that due to the presence of the $2\nu\beta\beta$ mode in conjunction with the energy resolution of only 300 keV this low background is very hard to reach and one has to scale up the other parameters of the experiment to fully cover the IH). Nevertheless, one can check that the background levels we have estimated here still correspond to a background dominated case.

5 Conclusions

The main focus of the present paper was put on testing the inverted neutrino mass hierarchy with neutrinoless double beta decay experiments. The maximal and (non-zero) minimal values of the effective mass are natural sensitivity goals for the experimental program.

We have stressed that the mixing parameter θ_{12} , the solar neutrino mixing angle, introduces an uncertainty of a factor of 2 on the minimal value of the effective mass. This implies an uncertainty of a factor of $2^2 = 4$ on the lifetime and $2^4 = 16$ on the combination of isotope mass, background level, energy resolution and measuring time. Given the long-standing problem of nuclear matrix element calculations we have taken a pragmatic point of view: to quantify the necessary half-lives to test and/or rule out the inverted hierarchy we have attempted to collect as many theoretical calculations as possible, and included their errors if available. The nuclear matrix elements we have compiled have been put on equal footing in what regards convention issues. We have used our compilation of NMEs to give the current limits on the effective mass of different isotopes, and to give the limits on the effective mass as a function of reached half-life. The isotope ^{100}Mo tends to look interesting, in the sense that with the same lifetime limit stronger constraints on the effective mass than for the other isotopes can be reached, an observation potentially interesting for upcoming experiments without a final decision on which isotope to use.

We finish by stressing once more that a precision determination of the solar neutrino mixing angle θ_{12} is of crucial importance to evaluate the physics potential of neutrinoless double beta decay experiments. A better knowledge of this parameter is desirable, and we hope to provide here additional motivation for further studies.

Acknowledgments

We thank Alexander Barabash, Jason Detwiler and Jorge Hirsch for helpful remarks. This work was supported by the ERC under the Starting Grant MANITOP and by the DFG in the Transregio 27 (A.D. and W.R.).

References

- [1] T. Tomoda, “Double beta decay,” *Rep. Prog. Phys.* **54** (1991) 53–126.
- [2] J. Vergados, “The Neutrinoless double beta decay from a modern perspective,” *Phys.Rept.* **361** (2002) 1–56, [hep-ph/0209347](#).
- [3] I. Avignone, Frank T., S. R. Elliott, and J. Engel, “Double Beta Decay, Majorana Neutrinos, and Neutrino Mass,” *Rev.Mod.Phys.* **80** (2008) 481–516, [arXiv:0708.1033 \[nucl-ex\]](#).
- [4] W. Rodejohann, “Neutrinoless Double Beta Decay in Particle Physics,” [arXiv:1011.4942 \[hep-ph\]](#).
- [5] S. Pascoli and S. Petcov, “The SNO solar neutrino data, neutrinoless double beta decay and neutrino mass spectrum,” *Phys.Lett.* **B544** (2002) 239–250, [hep-ph/0205022](#).
- [6] S. Petcov, “Theoretical prospects of neutrinoless double beta decay,” *Phys.Scripta* **T121** (2005) 94–101, [hep-ph/0504166](#).
- [7] T. Schwetz, M. A. Tortola, and J. W. F. Valle, “Three-flavour neutrino oscillation update,” *New J. Phys.* **10** (2008) 113011, [arXiv:0808.2016v3 \[hep-ph\]](#).
- [8] A. Faessler and F. Simkovic, “Double beta decay,” *J. Phys. G: Nucl. Part. Phys.* **24** (1998) 2139–2178.
- [9] J. Suhonen and O. Civitarese, “Weak-interaction and nuclear-structure aspects of nuclear double beta decay,” *Phys. Rep.* **300** (1998) 123–214.
- [10] J. Menéndez, A. Poves, E. Caurier, and F. Nowacki, “Disassembling the nuclear matrix elements of the neutrinoless $\beta\beta$ decay,” *Nucl. Phys. A* **818** (2009) 139–151, [arXiv:0801.3760v3 \[nucl-th\]](#).
- [11] J. Barea and F. Iachello, “Neutrinoless double- β decay in the microscopic interacting boson model,” *Phys. Rev. C* **79** (2009) 044301.
- [12] T. R. Rodriguez and G. Martinez-Pinedo, “Energy density functional study of nuclear matrix elements for neutrinoless $\beta\beta$ decay,” *Phys. Rev. Lett.* **105** (2010) 252503, [arXiv:1008.5260 \[nucl-th\]](#).
- [13] P. K. Rath, R. Chandra, K. Chaturvedi, P. K. Raina, and J. G. Hirsch, “Uncertainties in nuclear transition matrix elements for neutrinoless $\beta\beta$ decay within the projected-Hartree-Fock-Bogoliubov model,” *Phys. Rev. C* **82** (2010) 064310.
- [14] K. Zuber, “Consensus report of a workshop on matrix elements for neutrinoless double beta decay,” [nucl-ex/0511009](#).

- [15] A. Faessler, G. Fogli, E. Lisi, V. Rodin, A. Rotunno, *et al.*, “QRPA uncertainties and their correlations in the analysis of $0\nu\beta\beta$ decay,” *Phys.Rev.* **D79** (2009) 053001, [arXiv:0810.5733 \[hep-ph\]](#).
- [16] M. C. Chen, “The SNO liquid scintillator project,” *Nucl. Phys. Proc. Suppl.* **145** (2005) 65–68.
- [17] D. N. McKinsey and K. J. Coakley, “Neutrino detection with CLEAN,” *Astropart. Phys.* **22** (2005) 355–368, [astro-ph/0402007](#).
- [18] Y. Huang, R. Lanou, H. Maris, G. Seidel, B. Sethumadhavan, *et al.*, “Potential for Precision Measurement of Solar Neutrino Luminosity by HERON,” *Astropart.Phys.* **30** (2008) 1–11, [arXiv:0711.4095 \[astro-ph\]](#).
- [19] **LENS** Collaboration, R. Raghavan, “LENS, MiniLENS: Status and outlook,” *J.Phys.Conf.Ser.* **120** (2008) 052014.
- [20] A. Bandyopadhyay, S. Choubey, and S. Goswami, “Exploring the sensitivity of current and future experiments to $\Theta(\odot)$,” *Phys. Rev.* **D67** (2003) 113011, [hep-ph/0302243](#).
- [21] H. Minakata, H. Nunokawa, W. Teves, and R. Zukanovich Funchal, “Reactor measurement of $\theta(12)$: Principles, accuracies and physics potentials,” *Phys.Rev.* **D71** (2005) 013005, [hep-ph/0407326](#).
- [22] A. Bandyopadhyay, S. Choubey, S. Goswami, and S. Petcov, “High precision measurements of $\theta(\text{solar})$ in solar and reactor neutrino experiments,” *Phys.Rev.* **D72** (2005) 033013, [hep-ph/0410283](#).
- [23] S. Petcov and T. Schwetz, “Precision measurement of solar neutrino oscillation parameters by a long-baseline reactor neutrino experiment in Europe,” *Phys.Lett.* **B642** (2006) 487–494, [hep-ph/0607155](#).
- [24] A. B. Balantekin, “Significance of neutrino cross-sections for astrophysics,” *AIP Conf. Proc.* **1189** (2009) 11–15, [arXiv:0909.0226 \[hep-ph\]](#).
- [25] A. Friedland, C. Lunardini, and C. Pena-Garay, “Solar neutrinos as probes of neutrino matter interactions,” *Phys.Lett.* **B594** (2004) 347, [hep-ph/0402266](#).
- [26] C. H. Albright, A. Dueck, and W. Rodejohann, “Possible Alternatives to Tri-bimaximal Mixing,” *Eur. Phys. J.* **C70** (2010) 1099–1110, [arXiv:1004.2798 \[hep-ph\]](#).
- [27] J. Schechter and J. W. F. Valle, “Neutrinoless double- β decay in $SU(2)\times U(1)$ theories,” *Phys. Rev. D* **25** (1982) 2951–2954.

- [28] M. Lindner, A. Merle, and W. Rodejohann, “Improved limit on θ_{13} and implications for neutrino masses in neutrino-less double beta decay and cosmology,” *Phys. Rev. D* **73** (2006) 053005, [hep-ph/0512143](#).
- [29] J. Bernabeu, M. Blennow, P. Coloma, A. Donini, C. Espinoza, *et al.*, “EURONU WP6 2009 yearly report: Update of the physics potential of Nufact, superbeams and betabeams,” [arXiv:1005.3146](#) [[hep-ph](#)].
- [30] G. Audi, A. H. Wapstra, and C. Thibault, “The 2003 atomic mass evaluation: (II). Tables, graphs and references,” *Nuclear Physics A* **729** (2003) 337–676.
- [31] S. M. Bilenky, “Neutrinoless Double Beta-Decay,” (2010) , [arXiv:1001.1946](#) [[hep-ph](#)].
- [32] S. Cowell, “Scaling factor inconsistencies in neutrinoless double beta decay,” *Phys. Rev. C* **73** (2006) 028501, [nucl-th/0512012](#).
- [33] A. Smolnikov and P. Grabmayr, “Conversion of experimental half-life to effective electron neutrino mass in $0\nu\beta\beta$ decay,” *Phys. Rev. C* **81** (2010) 028502.
- [34] A. Faessler, G. L. Fogli, E. Lisi, V. Rodin, A. M. Rotunno, and F. Simkovic, “Quasiparticle random phase approximation uncertainties and their correlations in the analysis of $0\nu\beta\beta$ decay,” *Phys. Rev. D* **79** (2009) 053001.
- [35] F. Simkovic, A. Faessler, H. Muther, V. Rodin, and M. Stauf, “ $0\nu\beta\beta$ -decay nuclear matrix elements with self-consistent short-range correlations,” *Phys. Rev. C* **79** (2009) 055501, [arXiv:0902.0331v1](#) [[nucl-th](#)].
- [36] D.-L. Fang, A. Faessler, V. Rodin, and F. Simkovic, “Neutrinoless double- β decay of ^{150}Nd accounting for deformation,” *Phys. Rev. C* **82** (2010) 051301, [arXiv:1009.5579v1](#) [[nucl-th](#)].
- [37] O. Civitarese and J. Suhonen, “Nuclear Matrix Elements for Double Beta Decay in the QRPA approach: a critical review,” *Journal of Physics: Conference Series* **173** (2009) 012012.
- [38] J. G. Hirsch, O. Castanos, and P. Hess, “Neutrinoless double beta decay in heavy deformed nuclei,” *Nucl. Phys. A* **582** (1995) 124–140, [nucl-th/9407022](#).
- [39] F. Simkovic, G. Pantis, J. D. Vergados, and A. Faessler, “Additional nucleon current contributions to neutrinoless double β decay,” *Phys. Rev. C* **60** (1999) 055502.
- [40] F. Simkovic, A. Faessler, V. Rodin, P. Vogel, and J. Engel, “Anatomy of the $0\nu\beta\beta$ nuclear matrix elements,” *Phys. Rev. C* **77** (2008) 045503, [arXiv:0710.2055](#) [[nucl-th](#)].

- [41] G. A. Miller and J. E. Spencer, “A survey of pion charge-exchange reactions with nuclei,” *Ann. Phys.* **100** (1976) 562–606.
- [42] H. Feldmeier, T. Neff, R. Roth, and J. Schnack, “A unitary correlation operator method,” *Nucl. Phys. A* **632** (1998) 61–95, [nucl-th/9709038](#).
- [43] H. Mütter and A. Polls, “Correlations derived from modern nucleon-nucleon potentials,” *Phys. Rev. C* **61** (1999) 014304, [nucl-th/9908002](#).
- [44] H. Mütter and A. Polls, “Two-body correlations in nuclear systems,” *Prog. Part. Nucl. Phys.* **45** (2000) 243–334, [nucl-th/0001007](#).
- [45] C. Giusti, H. Mütter, F. D. Pacati, and M. Stauf, “Short-range and tensor correlations in the $^{16}\text{O}(e, e'pn)$ reaction,” *Phys. Rev. C* **60** (1999) 054608, [nucl-th/9903065](#).
- [46] A. S. Barabash, “75 years of double beta decay: yesterday, today and tomorrow,” [arXiv:1101.4502](#) [[nucl-ex](#)].
- [47] *See e.g., talks by A. Giuliani at BEYOND 2010 or by C. Nones at NOW 2010 .*
- [48] H. Ejiri *et al.*, “Spectroscopy of double-beta and inverse-beta decays from Mo-100 for neutrinos,” *Phys. Rev. Lett.* **85** (2000) 2917–2920, [nucl-ex/9911008](#).
- [49] **NEMO** Collaboration, A. Barabash, “Extrapolation of NEMO technique to future generation of 2beta-decay experiments,” *Czech.J.Phys.* **52** (2002) 575–581.
- [50] S. Umehara *et al.*, “Neutrino-less double- β decay of ^{48}Ca studied by $\text{CaF}_2(\text{Eu})$ scintillators,” *Phys. Rev. C* **78** (2008) 058501, [arXiv:0810.4746](#) [[nucl-ex](#)].
- [51] H. V. Klapdor-Kleingrothaus *et al.*, “Latest Results from the Heidelberg-Moscow Double Beta Decay Experiment,” *Eur. Phys. J. A* **12** (2001) 147–154, [hep-ph/0103062](#).
- [52] **NEMO** Collaboration, A. S. Barabash and V. B. Brudanin, “Investigation of double beta decay with the NEMO-3 detector,” [arXiv:1002.2862](#) [[nucl-ex](#)].
- [53] J. Argyriades *et al.*, “Measurement of the two neutrino double beta decay half-life of Zr-96 with the NEMO-3 detector,” *Nuclear Physics A* **847** (2010) 168–179, [arXiv:0906.2694](#) [[nucl-ex](#)].
- [54] F. A. Danevich *et al.*, “Search for 2β decay of cadmium and tungsten isotopes: Final results of the Solotvina experiment,” *Phys. Rev. C* **68** (2003) 035501.
- [55] C. Arnaboldi *et al.*, “Results from a search for the $0\nu\beta\beta$ -decay of ^{130}Te ,” *Phys. Rev. C* **78** (2008) 035502, [arXiv:0802.3439](#) [[hep-ex](#)].

- [56] R. Bernabei *et al.*, “Investigation of $\beta\beta$ decay modes in ^{134}Xe and ^{136}Xe ,” *Physics Letters B* **546** (2002) 23–28.
- [57] **NEMO** Collaboration, J. Argyriades *et al.*, “Measurement of the double- β decay half-life of ^{150}Nd and search for neutrinoless decay modes with the NEMO-3 detector,” *Phys. Rev. C* **80** (2009) 032501, [arXiv:0810.0248 \[hep-ex\]](#).
- [58] **IGEX** Collaboration, C. Aalseth *et al.*, “The IGEX Ge-76 neutrinoless double beta decay experiment: Prospects for next generation experiments,” *Phys.Rev.* **D65** (2002) 092007, [hep-ex/0202026](#).
- [59] H. Klapdor-Kleingrothaus and I. Krivosheina, “The evidence for the observation of neutrinoless double beta decay: The identification of neutrinoless double beta events from the full spectra,” *Mod.Phys.Lett.* **A21** (2006) 1547–1566.
- [60] S. Umehara, T. Kishimoto, I. Ogawa, R. Hazama, S. Yoshida, *et al.*, “CANDLES for double beta decay of Ca-48,” *J.Phys.Conf.Ser.* **39** (2006) 356–358.
- [61] I. Abt *et al.*, “A new 76Ge double beta decay experiment at LNGS,” [hep-ex/0404039](#).
- [62] **Majorana** Collaboration, C. E. Aalseth *et al.*, “The Majorana neutrinoless double-beta decay experiment,” *Phys. Atom. Nucl.* **67** (2004) 2002–2010, [hep-ex/0405008](#).
- [63] K. Zuber, “COBRA—double beta decay searches using CdTe detectors,” *Physics Letters B* **519** (2001) 1–7, [nucl-ex/0105018](#).
- [64] C. Arnaboldi *et al.*, “CUORE: a cryogenic underground observatory for rare events,” *Nucl. Instrum. Meth. A* **518** (2004) 775–798, [nucl-ex/0212053](#).
- [65] M. Danilov *et al.*, “Detection of very small neutrino masses in double-beta decay using laser tagging,” *Phys. Lett. B* **480** (2000) 12–18, [hep-ex/0002003](#).
- [66] Y. Takeuchi, “Recent status of the XMASS project,” *Prepared for ICHEP 04, Beijing, China, 16-22 Aug 2004*, (2004) 324–327.
- [67] **KamLAND** Collaboration, A. Terashima *et al.*, “R & D for possible future improvements of KamLAND,” *J.Phys.Conf.Ser.* **120** (2008) 052029.
- [68] **NEXT** Collaboration, . F. Granena *et al.*, “NEXT, a HPGXe TPC for neutrinoless double beta decay searches,” [arXiv:0907.4054 \[hep-ex\]](#).
- [69] N. Ishihara, T. Inagaki, T. Ohama, K. Omata, S. Takeda, *et al.*, “A Separation method of 0 neutrino and 2 neutrino events in double beta decay experiments with DCBA,” *Nucl.Instrum.Meth.* **A443** (2000) 101–107.
- [70] **SNO+** Collaboration, M. C. Chen, “The SNO+ Experiment,” [arXiv:0810.3694 \[hep-ex\]](#).

Appendix

Table 7: Required $0\nu\beta\beta$ decay half-life sensitivity (in 10^{27} yrs) in order to *exclude* the inverted hierarchy for different values of $\sin^2\theta_{12}$. For each value of $\sin^2\theta_{12}$ we present two values/ranges by varying the other parameters which determine the effective mass (Δm_A^2 , Δm_\odot^2 , $\sin^2\theta_{13}$) in their currently allowed 3σ region. Thereby, for each value of $\sin^2\theta_{12}$, the numbers in the first row correspond to the smallest possible half-lives while the numbers in the second row correspond to the largest half-lives. The values calculated using the pseudo-SU(3) NME for ^{150}Nd from Ref. [38] are (in the just described order) 2.34, 3.51, 3.77, 5.68, 8.90, 13.5 ($\times 10^{27}$ yrs).

Isotope	$\sin^2\theta_{12}$	half-life sensitivity to exclude IH [10^{27} yrs]					
		NSM [10]	Tü [35,36]	Jy [37]	IBM [11]	GCM [12]	PHFB [13]
^{48}Ca	0.270	9.88	-	-	-	1.27	-
		14.82	-	-	-	1.91	-
	0.318	15.93	-	-	-	2.05	-
		24.00	-	-	-	3.09	-
	0.380	37.62	-	-	-	4.84	-
		56.92	-	-	-	7.32	-
^{76}Ge	0.270	9.22	1.39 - 3.69	2.54 - 4.13	2.44 - 3.39	3.44	-
		13.82	2.08 - 5.53	3.80 - 6.20	3.65 - 5.08	5.16	-
	0.318	14.86	2.24 - 5.95	4.09 - 6.67	3.93 - 5.46	5.55	-
		22.38	3.37 - 8.96	6.16 - 10.04	5.92 - 8.22	8.35	-
	0.380	35.09	5.28 - 14.05	9.66 - 15.74	9.28 - 12.89	13.09	-
		53.08	7.99 - 21.26	14.62 - 23.82	14.03 - 19.50	19.81	-
^{82}Se	0.270	2.41	0.40 - 1.13	1.21 - 1.94	0.86 - 1.16	0.94	-
		3.61	0.60 - 1.70	1.82 - 2.91	1.29 - 1.74	1.41	-
	0.318	3.88	0.65 - 1.83	1.95 - 3.13	1.39 - 1.87	1.52	-
		5.85	0.98 - 2.75	2.94 - 4.71	2.09 - 2.82	2.29	-
	0.380	9.17	1.53 - 4.31	4.61 - 7.39	3.28 - 4.42	3.59	-
		13.88	2.32 - 6.52	6.98 - 11.17	4.97 - 6.68	5.43	-
^{96}Zr	0.270	-	1.51 - 3.31	0.83 - 1.05	1.26	0.25	0.67 - 1.60
		-	2.26 - 4.96	1.24 - 1.58	1.89	0.38	1.01 - 2.41
	0.318	-	2.43 - 5.34	1.34 - 1.70	2.03	0.41	1.08 - 2.59
		-	3.66 - 8.04	2.01 - 2.56	3.06	0.61	1.63 - 3.90
	0.380	-	5.73 - 12.60	3.16 - 4.01	4.79	0.96	2.56 - 6.11
		-	8.67 - 19.06	4.77 - 6.07	7.25	1.45	3.87 - 9.24

Table 7: (continued)

Isotope	$\sin^2\theta_{12}$	NSM	Tübingen	Jyväskylä	IBM	GCM	PHFB
^{100}Mo	0.270	-	0.28 - 1.03	0.67 - 1.08	0.58 - 0.75	0.40	0.17 - 0.47
		-	0.42 - 1.55	1.01 - 1.62	0.88 - 1.12	0.60	0.26 - 0.70
	0.318	-	0.46 - 1.66	1.08 - 1.74	0.94 - 1.20	0.65	0.28 - 0.76
		-	0.69 - 2.51	1.63 - 2.62	1.42 - 1.81	0.98	0.42 - 1.14
	0.380	-	1.08 - 3.93	2.56 - 4.11	2.23 - 2.84	1.53	0.66 - 1.78
		-	1.63 - 5.94	3.88 - 6.22	3.37 - 4.30	2.32	0.99 - 2.70
^{110}Pd	0.270	-	-	-	2.47	-	0.41 - 1.14
		-	-	-	3.70	-	0.61 - 1.71
	0.318	-	-	-	3.98	-	0.66 - 1.84
		-	-	-	5.99	-	0.99 - 2.77
	0.380	-	-	-	9.39	-	1.55 - 4.34
		-	-	-	14.21	-	2.35 - 6.57
^{116}Cd	0.270	-	0.48 - 1.56	0.63 - 1.09	1.27	0.44	-
		-	0.72 - 2.34	0.95 - 1.64	1.90	0.66	-
	0.318	-	0.78 - 2.51	1.02 - 1.76	2.04	0.71	-
		-	1.17 - 3.79	1.54 - 2.66	3.08	1.07	-
	0.380	-	1.83 - 5.93	2.41 - 4.16	4.83	1.68	-
		-	2.77 - 8.98	3.65 - 6.30	7.30	2.54	-
^{124}Sn	0.270	2.59	-	-	-	0.77	-
		3.88	-	-	-	1.15	-
	0.318	4.18	-	-	-	1.24	-
		6.29	-	-	-	1.87	-
	0.380	9.86	-	-	-	2.93	-
		14.92	-	-	-	4.43	-
^{130}Te	0.270	1.58	0.37 - 1.09	0.62 - 0.91	0.67 - 0.97	0.42	0.42 - 1.24
		2.37	0.55 - 1.64	0.93 - 1.37	1.01 - 1.46	0.63	0.63 - 1.86
	0.318	2.55	0.59 - 1.76	1.00 - 1.47	1.08 - 1.57	0.68	0.68 - 2.00
		3.83	0.89 - 2.65	1.51 - 2.22	1.63 - 2.37	1.02	1.03 - 3.01
	0.380	6.01	1.40 - 4.16	2.37 - 3.48	2.56 - 3.71	1.60	1.61 - 4.72
		9.09	2.11 - 6.29	3.58 - 5.26	3.88 - 5.61	2.43	2.44 - 7.14
^{136}Xe	0.270	2.19	0.84 - 3.59	1.34 - 1.86	0.94	0.60	-
		3.29	1.26 - 5.38	2.01 - 2.78	1.40	0.89	-
	0.318	3.54	1.36 - 5.78	2.16 - 2.99	1.51	0.96	-
		5.33	2.04 - 8.71	3.25 - 4.51	2.27	1.45	-
	0.380	8.35	3.21 - 13.65	5.10 - 7.07	3.56	2.27	-
		12.63	4.85 - 20.65	7.72 - 10.70	5.39	3.43	-

Table 7: (continued)

Isotope	$\sin^2\theta_{12}$	NSM	Tübingen	Jyväskylä	IBM	GCM	PHFB
^{150}Nd	0.270	-	0.20	-	0.28 - 0.44	0.81	0.17 - 0.60
		-	0.30	-	0.42 - 0.66	1.21	0.26 - 0.90
	0.318	-	0.32	-	0.46 - 0.71	1.30	0.28 - 0.97
		-	0.48	-	0.69 - 1.06	1.96	0.42 - 1.46
	0.380	-	0.76	-	1.08 - 1.67	3.07	0.66 - 2.29
		-	1.14	-	1.63 - 2.52	4.65	0.99 - 3.47

Table 8: Same as Table 7, but here the required $0\nu\beta\beta$ decay half-life sensitivity in order to *touch* the inverted hierarchy is given. For the pseudo-SU(3) NME for ^{150}Nd we get the values 0.49, 0.72 ($\times 10^{27}$ yrs).

Isotope	half-life sensitivity to touch IH [10^{27} yrs]					
	NSM [10]	Tübingen [35,36]	Jyväskylä [37]	IBM [11]	GCM [12]	PHFB [13]
^{48}Ca	2.05	-	-	-	0.26	-
	3.03	-	-	-	0.39	-
^{76}Ge	1.91	0.29 - 0.77	0.53 - 0.86	0.51 - 0.70	0.71	-
	2.82	0.42 - 1.13	0.78 - 1.27	0.75 - 1.04	1.05	-
^{82}Se	0.50	0.08 - 0.24	0.25 - 0.40	0.18 - 0.24	0.20	-
	0.74	0.12 - 0.35	0.37 - 0.59	0.26 - 0.36	0.29	-
^{96}Zr	-	0.31 - 0.69	0.17 - 0.22	0.26	0.05	0.14 - 0.33
	-	0.46 - 1.01	0.25 - 0.32	0.39	0.08	0.21 - 0.49
^{100}Mo	-	0.06 - 0.21	0.14 - 0.22	0.12 - 0.16	0.08	0.04 - 0.10
	-	0.09 - 0.32	0.21 - 0.33	0.18 - 0.23	0.12	0.05 - 0.14
^{110}Pd	-	-	-	0.51	-	0.08 - 0.24
	-	-	-	0.76	-	0.12 - 0.35
^{116}Cd	-	0.10 - 0.32	0.13 - 0.23	0.26	0.09	-
	-	0.15 - 0.48	0.19 - 0.33	0.39	0.13	-
^{124}Sn	0.54	-	-	-	0.16	-
	0.79	-	-	-	0.24	-
^{130}Te	0.33	0.08 - 0.23	0.13 - 0.19	0.14 - 0.20	0.09	0.09 - 0.26
	0.48	0.11 - 0.33	0.19 - 0.28	0.21 - 0.30	0.13	0.13 - 0.38
^{136}Xe	0.46	0.17 - 0.74	0.28 - 0.39	0.19	0.12	-
	0.67	0.26 - 1.10	0.41 - 0.57	0.29	0.18	-

Table 8: (continued)

Isotope	NSM	Tübingen	Jyväskylä	IBM	GCM	PHFB
^{150}Nd	-	0.04	-	0.06 - 0.09	0.17	0.04 - 0.13
	-	0.06	-	0.09 - 0.13	0.25	0.05 - 0.18